Atmos. Meas. Tech. Discuss., 3, 2651–2680, 2010
www.atmos-meas-tech-discuss.net/3/2651/2010/
doi:10.5194/amtd-3-2651-2010
© Author(s) 2010. CC Attribution 3.0 License.

Atmospheric Measurement Techniques Discussions

This discussion paper is/has been under review for the journal Atmospheric Measurement Techniques (AMT). Please refer to the corresponding final paper in AMT if available.

Satellite remote sensing of Asian aerosols: a case study of clean, polluted and dust storm days

K. H. Lee[1] **and Y. J. Kim**[2]

[1]Dept. of Satellite Geoinformatics Engineering, Kyungil University, Geongsan 712-701, Republic of Korea
[2]Advanced Environmental Monitoring Research Center, Department of Environmental Science and Engineering, Gwangju Institute of Science and Technology, 1 Oryong dong, Buk-gu, Gwangju 500-712, Republic of Korea

Received: 30 March 2010 – Accepted: 24 April 2010 – Published: 24 June 2010

Correspondence to: K. H. Lee (khlee@kiu.ac.kr)

Published by Copernicus Publications on behalf of the European Geosciences Union.

Abstract

Satellite-based aerosol observation is a useful tool for the estimation of microphysical and optical characteristics of aerosol during more than three decades. Until now, a lot of satellite remote sensing techniques have been developed for aerosol detection. In East Asian region, the role of satellite observation is quite important because aerosols originating from natural and man-made pollution in this region have been recognized as an important source for regional and global scale air pollution. However, it is still difficult to retrieve aerosol over land because of the complexity of the surface reflection and complex aerosol composition, in particular, aerosol absorption. In this study, aerosol retrievals using Look-up Table (LUT) based method was applied to MODerate Resolution Imaging Spectroradiometer (MODIS) Level 1 (L1) calibrated reflectance data to retrieve aerosol optical thickness (AOT) over East Asia. Three case studies show how the methodology works to identify those differences to obtain a better AOT retrieval. The comparison between the MODIS and Aerosol Robotic Network (AERONET) shows better results when the suggested methodology using the cluster based LUTs is applied (linear slope=0.94, R=0.92) than when operational MODIS aerosol products are used (linear slope=0.78, R=0.87). In conclusion, the suggested methodology is shown to work well with aerosol models acquired by statistical clustering the observation data in East Asia.

1 Introduction

Atmospheric aerosols originate either from natural sources (dust, volcanic, or sea salt, etc.) or from anthropogenic sources (fires, sulfates, soot, etc.). Due to their very high spatio-temporal variability and optical properties, they are one of the main sources of uncertainty in climate change (IPCC, 2007). Observation from satellites, being global and quasi-continuous, has been a major tool for aerosol studies. Until now, various techniques of satellite remote sensing in the visible wavelengths have been widely

AMTD
3, 2651–2680, 2010

used to obtain a characterization of aerosols and their effect on solar radiation (King et al., 1999; Lee et al., 2009). Not only knowledge of the microphysical and optical properties of aerosols on the radiative transfer is needed for the retrieval of the aerosols, but also exact estimation of surface reflectance provides a way to retrieve reasonable aerosol characteristics. The uncertainties and discrepancies among different retrieval algorithms have been conducted (Kokhanovsky et al., 2007, 2009a, b; Mishchenko et al., 2007) and some insights were studied (Jeong et al., 2005; Liu and Mishchenko, 2008; Kinne et al., 2006). However, major improvements in the accuracy and spatial resolution of the satellite products are still required for air quality applications in urban areas (Li et al., 2005).

As a measured value of aerosol loading, aerosol optical thickness (AOT) is a basic optical property derived from many Earth observation satellites such as the Advanced Very High Resolution Radiometer (AVHRR) (Rao et al., 1989; Stowe, 1991), the MODerate resolution Imaging Spectro-radiometer (MODIS) (Kaufman et al., 1997a), the Multi-angle Imaging Spectro-Radiometer (MISR) (Diner et al., 1998), and the Sea-viewing Wide Field-of-view Sensor (SeaWiFS) (Gordon and Wang, 1994; von Hoyningen-Huene et al., 2003), etc. AOT is directly related to the atmospheric aerosol load, which is the principal variable describing the effect of aerosols on radiative transfer in the Earth's atmosphere. Remote sensing of aerosols over land is particularly important because the sources of most aerosols (mainly anthropogenic aerosols) are located in land. It is very useful to identify sources, understand transformations in the atmosphere, and estimate the anthropogenic contribution. A major problem in aerosol retrieval over land is that the surface reflectance is not only higher than that over the ocean in general, but it also varies spatially and temporally. An inaccurate surface reflectance estimation of 0.01 can result in an uncertainty of 10% in AOT estimation (Soufflet et al., 1997; Kaufman et al., 1997b). To date, aerosol retrieval over East Asia has not been thoroughly studied. This paper attempts to rectify this situation through the statistical analysis of retrievals of AOT obtained from the satellite radiance measurements.

AMTD
3, 2651–2680, 2010

This study presents a validation of aerosol retrieval based on interactive look-up tables (LUTs) and comparison with operational aerosol products such as MODIS level 2 and The Aerosol Robotic Network (AERONET) sun-sky radiometer measured AOT that better represents aerosols at a specific place and time. We develop LUTs by means of statistical classification method, which is defined in previous work (Omar et al., 2005). For this classification, aerosol optical properties were obtained from AERONET sun-sky radiometer data archive (AERONET, 2010). Aerosol retrieval is then processed by a step forward from the classified aerosol models and has the advantage of representing a more accurate retrieval of the AOT. The retrieved AOT from the 1 km resolution from MODIS L1 calibrated reflectance data using this method is compared with MODIS Level 2 and AERONET AOT measured from the ground.

This paper is organized as follows. Section 2 describes the LUTs construction with cluster analysis and the sensitivity tests. Section 3 describes the data set used to retrieve the AOT and the details of the retrieval algorithm. The results of aerosol retrievals from MODIS and their consistency with AERONET data are discussed in Sect. 4. Finally, conclusions are given in Sect. 5.

2 Aerosol models

Aerosol retrieval based on LUTs highly depends on the aerosol models used in the radiative transfer code. Aerosol models can be acquired from well known global climatology (Shettle and Fenn, 1979; d'Almeda et al., 1992; Hess et al., 1998). Nevertheless, aerosol microphysical and optical properties based on in-situ measurement or sun photometry describe real atmospheric conditions (Dubovik and King, 2000). Since aerosols are mainly originated from transport of local air masses and nonsystematic events such as biomass burning (BB), re-suspension, and human activities, these variations lead to diverse aerosol characteristics. The representative aerosol type at a region of interest can be found by the occurrence of a typical type of aerosol at that location if an adequately large sample is used for calculations. Therefore, assigning of

AMTD
3, 2651–2680, 2010

typical aerosol microphysical and optical properties to a given location based on a long term average has significant shortcomings (Sheridan et al., 2001).

In the East Asia, our region of interest, atmospheric aerosols originated from BB and human activities are recognized as an important source of regional- and global-scale pollution (Streets et al., 2003; Wenig et al., 2003). Furthermore, the long-range transport of aerosols occurs frequently depending on the meteorological conditions, and affects air quality over downwind areas. These transported pollutants contain not only mineral dust, but pollution aerosol consisting of sulfate, nitrate and carbonaceous particles (Song et al., 2008). To develop a type-specific aerosol models which include aerosol microphysics and optical properties over the East Asia, the AERONET database with very fine temporal resolution is used (Holben et al., 1998; Dubovik and King, 2000). A detailed description of the products is found in the documents of description (see AERONET inversion, 2010; AERONET criteria, 2010).

The study area of this paper (20° N–50° N, 100° E–150° E), is shown in Fig. 1. Locations of nineteen AERONET sites in the study area, Anmyon, Beijing, Chen-Kung_Univ, Gosan, Gwangju, Hefei, Hong Kong Hok Tsui (HKHT), Hong Kong Polytechnic University (HKPU), Jeju, Lulin, National Central University (NCU), Noto, Osaka, Seoul, Shirahama, Taihu, Xianghe, Xinglong, Yulin, and Ussuriysk, are also shown. Post-calibrated and quality assured Level 2.0 AERONET inversion data since 1998, such as AOT, size distribution, single scattering albedo (SSA), asymmetry parameter (g), refractive indices, etc. are available for grouping large data sets into some categories using the cluster analysis technique (cf. Kaufman and Rousseeuw, 1990; Omar et al., 2005).

After clustering, six aerosol types are determined in this study. If cluster analysis uses two or three clusters, similar type of aerosol may lose their characteristics independently to form one or two new clusters. As we go to a larger number of clusters, the members of the main clusters are relatively unchanged. Six clusters provided the largest number of clusters in which each cluster had a reasonable number of categories. The numbers of cases in each cluster are listed in Table 1. 83% of the records are grouped in category 1, 3, and 4. Category 2, 5, and 6 cluster has the 16.9% of

AMTD
3, 2651–2680, 2010

the total number of case. It is therefore possible for a region of interest to belong to more than one category. Table 2 shows the aerosol and microphysical properties, as well as the number of records for each cluster. Each aerosol model has somewhat different values for refractive indices at particular wavelengths, median particle radius, standard deviation of size distribution, and other optical properties. The aerosol size distribution used in this study is the volume size distribution provided by the AERONET inversion algorithm. The best fit for this size distribution data is a bimodal lognormal size distribution described by Eq. (1),

$$\frac{dV}{d\ln r} = \frac{C_{\text{fine}}}{\sqrt{2\pi}\cdot S_{\text{fine}}}\exp\left[\frac{(\ln R - \ln R_{\text{fine}})^2}{2(S_{\text{fine}})^2}\right] + \frac{C_{\text{coarse}}}{\sqrt{2\pi}S_{\text{coarse}}}\exp\left[\frac{(\ln R - \ln R_{\text{coarse}})^2}{2(S_{\text{coarse}})^2}\right] \quad (1)$$

where C, R, and S are total mode volume ($\mu m^{-3}/\mu m^{-2}$), median radius, and geometric standard deviation, respectively. The subscripts of *fine* and *coarse* denote fine and coarse modes. This partition of the size distribution into fine and coarse modes yields six parameters by which the size distribution can be described.

Figure 2 compares size distribution, SSA, g for the six clustered aerosol models. Size distributions show that the values of $dV/d\ln r$ vary significantly for different categories. Category 1–4 have larger fine mode compared with category 5–6 and SSA values vary from 0.90 to 0.93 at 440 nm. Much of the differences in absorption magnitude between two categories may be attributed to differences in the relative percentage of absorbing aerosols which are generally finer particulates. This indicates that these aerosol types are more likely to experience continental or urban/industrial pollution more than other aerosol types. The highest absorption (lowest SSA) was shown for category 3–4. The absorption for category 5–6 was shown for the large coarse mode with similar SSA and g values with the strongest spectral dependence. In this classification, category 5–6 may be referred to dusty aerosols.

AMTD
3, 2651–2680, 2010

3 Look-up tables

A LUT is used for the aerosol retrieval in this study. The LUT contains several sets of the pre-computed reflectances for each of the MODIS seven visible channel wavelengths (0.47 µm, 0.55 µm, 0.66 µm, 0.865 µm, 1.24 µm, 1.63 µm, and 2.13 µm). The reflectances in the LUT are computed using clustered aerosol models that represent realistic possibilities for the aerosol properties of a vertical column of atmosphere. Those aerosol models are based on real measurements involving sun photometer data as explained Sect. 2. Basically, the LUTs describe the relationships between satellite receiving radiance and the AOT for a given atmospheric and surface condition. In this study, LUTs were calculated by the Santa Barbara DISORT Atmospheric Radiative Transfer (SBDART) (Ricchiazzi et al., 1988) code for the retrieval. The SBDART code can calculate solar flux as well as radiance at different atmospheric height for the solar illumination and satellite observation geometry. For SBDART running, AOT at 550 nm, spectral aerosol extinction, SSA, and g are required. To construct LUTs with different aerosol types, six aerosol models determined in Sect. 2 are used as an input data for SBDART.

Examples of SBDART calculations are shown in Fig. 3. Each curve represents aerosol reflectance as a function of AOT at 550 nm. Under dark surface condition (surface albedo=0), aerosol reflectance (ρ_{Aer}) from SBDART calculations can be formulated as follows:

$$\rho_{\mathrm{Aer}}(\theta_0,\theta_S,\Theta) = \rho_{\mathrm{TOA}}(\theta_0,\theta_S,\Theta) - \rho_{\mathrm{Ray}}(\theta_0,\theta_S,\Theta) \quad (2)$$

where, ρ_{TOA}, ρ_{Ray} are the TOA and Rayleigh reflectance, respectively. ρ_{Ray} can be obtained when aerosols do not exist (AOT=0). θ_0, θ_S, Θ represent sun zenith angle, satellite viewing angle, and relative azimuth angle between sun and satellite. Reflectance can be calculated by the normalization of radiance $L(\lambda)$ to the extraterrestrial irradiance $F_0(\lambda)$:

$$\rho(\lambda) = \frac{\pi \cdot L(\lambda)}{F_0 \cdot \cos\theta_0} \quad (3)$$

AMTD
3, 2651–2680, 2010

The LUT was calculated up to an AOT of 5.0 (0.0, 0.2, 0.4, 0.8, 1.0, 1.4, 1.8, 2.2, 3.0, 4.0, and 5.0). Geometrical inputs are θ_0=0°∼80°(Δ=10°), θ_S=0°∼80°(Δ=5°), and Θ=0°∼170° (Δ=10°), respectively. Therefore, total number of calculation is 6 aerosol models×7 bands×11 AOTs×9 θ_0×17θ_S×18Θ=1 272 348.

Aerosol reflectance increases strongly with increasing AOT and this increasing rate is different. This means selection of aerosol model can lead to a high variation in the AOT. If algorithm chooses wrong aerosol model, the largest differences of ±67% in the retrieved AOT are anticipated when the real AOT of 4.0 is assumed. Yet, this makes a difference for lower AOT (<0.2), where the aerosol reflectance is about 0.03, of ±0.01 (10%) in the retrieved AOT. Thus, the aerosol model has an important influence on the retrieved AOT and LUTs for different aerosol types are required.

4 Aerosol retrieval method

In this study, aerosol retrieval algorithm over land uses the dark target approach (Kaufman et al., 1997a, b), spectral mixed and separation technique (von Hoyningen et al., 2003), spectral shape matching (Lee et al., 2007). This is a valid assumption for land surfaces. The method is part of aerosol retrieval procedure for SeaWiFS (Lee et al., 2004) and MODIS (Lee et al., 2007) developed by the Advanced Environment Monitoring Research Center (ADEMRC) of the Gwangju Institute of Science & Technology (GIST), called SaTellite Aerosol Retrieval (STAR). In the algorithm, the blue channel of satellite instrument is used for separation between surface and atmosphere because surface reflectance is relatively low in this spectral region. AOT is then determined by using adequate LUT. However, by LUT with wrong aerosol this leads to an overestimation or underestimation of the AOT. To avoid this problem, recent operational algorithms (Kaufman and Tanre, 1998; Khan et al., 2005) use the best combination LUT with fine and coarse mode aerosol model based on global aerosol climatology. This study is focusing on an improvement of the aerosol model to reflect local characteristics and its integration within the retrieval procedure. The aerosol retrieval based

AMTD
3, 2651–2680, 2010

on LUTs described in Sect. 2 for the East-Asian region has been applied for MODIS data. To distinguish between cloudy and cloud free pixels from MODIS observations we used MOD35 cloud screening approach (Ackerman et al., 1998). Comparisons of the retrieved AOT results with other measurements are shown in Sect. 4.

An overview of the aerosol retrieval process is presented in Fig. 4. The following equation has been introduced to determine aerosol reflectance by separating surface reflectance and Rayleigh path radiance from TOA reflectance (Kaufman et al., 1997a).

$$\rho_{\mathrm{Aer}}(\theta_0,\theta_S,\phi) = \rho_{\mathrm{TOA}}(\theta_0,\theta_S,\phi) - \rho_{\mathrm{Ray}}(\theta_0,\theta_S,\phi) - \frac{T_{\mathrm{Tot}}(\theta_0)\cdot T_{\mathrm{Tot}}(\theta_S)\cdot \rho_{\mathrm{Surf}}(\theta_0,\theta_S)}{1-\rho_{\mathrm{Surf}}(\theta_0,\theta_S)\cdot r_{\mathrm{Hem}}(\tau_{\mathrm{Tot}},g)} \quad (4)$$

where τ_{Tot} represent total optical thickness, $T_{\mathrm{Tot}}(m_0)$ the total atmospheric transmittance, $\rho_{\mathrm{Surf}}(\theta_0,\theta_S)$ the surface reflectance, and $r_{\mathrm{Hem}}(\tau_{\mathrm{Tot}},g)$ the hemispheric reflectance, respectively. Total transmissions and hemispheric reflectance are determined by parameterization derived from radiative transfer calculations (see von Hoyningen-Huene et al., 2007). Thus, aerosol reflectance can be obtained by subtracting Rayleigh and surface terms from TOA reflectance. The aerosol reflectance also contains the molecular-aerosol scattering coupling term. The accurate estimation of surface reflectance is therefore required for aerosol retrieval from satellite data. A linear mixing model between vegetation and bare soil spectra estimates the surface reflectance (von Hoyningen et al., 2003) were used to estimate surface reflectance in the following manner:

$$\rho_{\mathrm{Surf}}(\lambda) = w\left[\mathrm{NDVI}_{\mathrm{SW}}\cdot\rho_{\mathrm{Veg}}(\lambda) + (1-\mathrm{NDVI}_{\mathrm{SW}})\cdot\rho_{\mathrm{Soil}}(\lambda)\right] \quad (5)$$

where w is the weighting factor for the level of the surface reflectance at 0.66 µm. λ is wavelength. $\rho_{\mathrm{Veg}}(\lambda)$ and $\rho_{\mathrm{Soil}}(\lambda)$ are the spectral reflectances of "green vegetation" and "bare soil", respectively. Detail description was discussed in von Hoyningen et al. (2003). $\mathrm{NDVI}_{\mathrm{SW}}$is the vegetation index representative of the vegetation fraction in each pixel (see Levy et al., 2007). In this manner, the algorithm retrieves AOT by separating the aerosol reflectance from the satellite receiving radiance. The main

AMTD
3, 2651–2680, 2010

problem is the selection and consideration of the variability of aerosol models. To select an optimum aerosol model, spectral shape fitting is used in this study. This procedure compares aerosol reflectance from satellite observation and from various LUTs at a given sun-satellite geometry. Similar approaches are found in previous studies (e.g. Kaufman and Tanré, 1998; Costa et al., 1999; Torricella et al., 1999; Lee et al., 2007). Basically, this method can determine the most appropriate aerosol model by finding the minimum difference term (χ^2) that describes the agreement between the measured and calculated values. The error can be expressed as the following equation:

$$\chi^2 = \frac{1}{n}\sum_{i=1}^{n}\left(\frac{\rho^m_{\mathrm{Aer}}(\lambda_i) - \rho^c_{\mathrm{Aer}}(\lambda_i)}{\rho^m_{\mathrm{Aer}}(\lambda_i)}\right) \quad (6)$$

where n is the number of selected wavelengths, superscripts m and c represent the measured and calculated, respectively. Fitting is done at the selected wavelengths of 0.47, 0.55 and 0.66 μm in order to minimize interference by gas absorption and surface reflectance. The best aerosol model is then determined by iteration as shown in Fig. 4.

5 Sensitivity study

AOT, one of major parameters affecting to the radiative transfer calculations, is the basic output parameter from satellite data retrieval. For finding the theoretical relationship between satellite receiving radiance and AOT, the input parameters for radiative transfer code include AOT at 550 nm, SSA, g, etc. The quality of these data depends directly on the quality of the retrieved AOT. The purpose of this chapter is to provide the sensitivity of the retrieved AOT changes with respect to the error-causing input parameters. The sensitivity test results show the importance of accurate information for the SSA and g in the satellite retrieval of AOT.

We simulated with the assumed error range of the input parameter and compute the resulting error on the retrieved AOT. The sensitivity study was performed to determine the impact of an error on the each parameter, by comparing with controlled values

AMTD
3, 2651–2680, 2010

which are assumed as SSA=0.91 and g=0.70. The term "error" used in this study can be expressed as the relative mean square error (RMSE).

$$\Delta\tau_{\varepsilon} = \sqrt{\frac{\sum_{i=0}^{n}(\tau_C - \tau_{\text{ref}})^2}{n-1}} \tag{7}$$

where τ_C and τ_{ref} are calculated, and referenced AOT by controlled value. n is the number of calculations. The terms on the right side of Eq. (7) were estimated by calculating the SBDART response to realistic errors in the input parameters. Uncertainty on the retrieved AOT from AERONET cluster based LUTs will absolutely affect the accuracy of the dataset. In Fig. 5, the error of AOT retrieval increases as a function of the error of SSA and g.

One of important parameters is SSA which is an important source of uncertainty in the retrieval of AOT. Highly variable SSA in East Asian region, typically from 0.88 up to 0.97, shows the importance of using accurate information for the single scattering albedo property of the aerosol. Since errors in AERONET derived SSA were estimated to be around 0.03 (AOT>0.2) and 0.05–0.07 (AOT<0.2) (Dubovik et al., 2000), these errors in SSA could be included in our approach. To estimate the error on AOT retrieval, errors within ±0.05 SSA were applied for radiative transfer simulations. As shown on Fig. 5a, the error of SSA could translate to higher error on retrieved AOT because of increased/decreased radiance when SSA is increasing/decreasing. This plot can be interpreted as a linear fitted line of dAOT(%)=−16.44 dSSA (R=0.97). Therefore, uncertainty of 0.05 SSA can cause uncertainty in the retrieved AOT by as much as 0.8.

The error caused by g is also important in the radiative transfer calculation. Uncertainties in the retrieval of g from AERONET data are in the range 3–5% (see Andrews et al., 2006). In this error range, the error ranges within ±0.05 are considered to estimate the AOT retrieval error. The resulting error is large with respect to increasing change of g. Liner fit as shown in Fig. 5b is dAOT(%)=12.37 dg (R=0.99), the AOT error caused by g is substantially lower than the error by SSA. The g in East Asia varies

AMTD
3, 2651–2680, 2010

from 0.72 to 0.76 at 440 nm. This means that 5% error (~0.04) of g can induce an error of around 0.49 in the retrieved AOT.

6 Aerosol retrieval

The AOT is highly depends on the intensity of scattering as well as absorption by aerosols. This quantity can be retrieved by the algorithm described in Sect. 4. In this section, three different cases of clear sky, local polluted, and dust storm in Northeast China region are studied. For the comparison of retrieved AOT and other measurements (e.g. collection 5 MODIS L2 AOT and AERONET AOT), linear regression analysis with collocated data from long-term and multi-locations was employed. There are twenty AERONET stations in East Asia as shown in Fig. 1.

Spatial distributions of the AOT at 550 nm obtained by this study (left column), called as MODIS STAR (MSTAR) AOT and MOD04 L2 AOT (right column) for the three aerosol cases are shown in Fig. 6. In this figure, two different MODIS AOTs with MOD04 fine mode fraction (FMF) and MSTAR aerosol class are plotted for clean, pollution, and dust cases. These aerosol classes are visually shown well in the RGB color composite images as different colors. 1km resolution AOT values obtained by this study provide much more detail than those from the 10 km resolution MOD04 L2 AOT. It is interesting to note that, although MOD04 shows a similar distribution of AOT, it does not show clear sky and heavy dust cases well. The white pixels in the imagery are null data removed from the algorithm because of clouds, bright surface, or heavy aerosol load. Although MOD04 shows a similar distribution of AOT, it shows relatively higher than AERONET results (see Table 3), probably due to the uncertainty of surface reflectance and aerosol model. Earlier studies (Li et al., 2007; Mi et al., 2007) showed similar overestimation of MOD04 AOT. During polluted and dust conditions the absorbing aerosols can absorb solar radiation resulting in an increase of AOT. In these heavy aerosol layers show MOD04 AOT of 1~2 but FMF shows near zero, that is, aerosol retrieval with a selected LUT may wrong. In this case, MSTAR aerosol type classification

AMTD
3, 2651–2680, 2010

shows red and orange color for dust predominant scene. However, somewhat erroneous result over very bright surface (e.g. desert region in North China) that large dust model (CAT-6) is detected. Although the sensitivity of TOA reflectance to aerosol type is less for smaller AOT (see Fig. 3) the information from aerosol class map must be used with caution. Improvement and verification of the retrieved aerosol class need further investigation.

To estimate the validity of aerosol retrieval in this study, it is necessary to compare results with other independent data derived from direct radiation measurements. Figure 7a shows the correlation between MSTAR AOT and AERONET sun-sky radiometer-derived AOT. For this comparison, MODIS pixels within 50 km close to each AERONET station were selected while AERONET data within 30 min of satellite overpassing time were taken (see Ichoku et al., 2004). These spatially averaged MSTAR AOTs and temporally averaged AERONET AOTs were then used for validation of satellite determined AOT retrieval. A good agreement with a linear slope of 0.94 and correlation coefficient R of 0.92 is found in Fig. 4a. Figure 4b shows a correlation between MOD04 AOT and AERONET sun-sky radiometer-derived AOT (linear slope=0.78; R=0.87), which indicates that MSTAR AOT over the study area yielded better results than MOD04 AOT.

Figure 8 shows the AOD map within 200 km×100 km rectangular including two AERONET sites of Beijing and Xianghe where larger AOT was observed. Comparison of results for MSTAR AOT and AERONET AOT at Beijing and Xinghe sites is summarized in Table 3. The mean AOT estimated from clear, hazy and dust conditions are found to be 0.23, 0.99, and 2.48, which corroborates well the AERONET AOTs (clean: 0.11, polluted: 1.09, dust: 2.49), respectively. AOTs increase by a factor of 9 to 20 during polluted and dust conditions with respect to the AOT estimated during clean periods. For clean case, larger AOT value compared with the AERONET results probably due to underestimated surface reflectance separated from the satellite signal. The point to be emphasized is that the suggested method, even for clear sky or heavy aerosols in the atmosphere, was enough to be identified by this study. As shown in Sect. 5, the aerosol model plays an important role in the retrieval of AOT, and the use

AMTD
3, 2651–2680, 2010

of LUTs based on cluster analysis showed significant potential to retrieve AOT over land. Further analysis of the surface reflectance over study areas could increase the accuracy even for bright surface.

7 Summary and conclusion

This study presented a construction of LUTs based on statistical cluster with AERONET database. By clustering, six aerosol types were determined and they provided information on major aerosol types in the study area. Each aerosol class shows independent aerosol microphysics and optics (particle size distribution, SSA, and g). Moreover, the results are quite different from known global aerosol model such as OPAC (Hess et al., 1998). This indicates that specified local aerosol types are more likely appropriate to apply LUTs based aerosol retrieval.

For aerosol retrieval from satellite data, the best aerosol model selection in the algorithm was used. Our main concern is the selection and consideration of the variability of aerosol models since a selection of wrong aerosol may lead to an overestimation or underestimation of the AOT. Sensitivity studies show that the quality of the AOT retrieved from satellite is directly related to the accuracy of the assumed aerosol optical property, such as SSA and g. Uncertainty of 0.05 SSA can cause uncertainty in the retrieved AOT by as much as 0.8. The AOT error caused by g is substantially lower than the error by SSA. 5% error (~0.04) of g can induce an error of around 0.49 in the retrieved AOT.

The case studies of the clean, polluted and Asian dust show the potential of the suggested methodology to retrieve well enough level of the AOT by their successful selection of aerosol model for the region. In general, a good agreement with a linear slope of 0.94 and correlation coefficient R of 0.92 is found and this result is comparable with a correlation between MOD04 AOT and AERONET sun-sky radiometer-derived AOT (liner slope=0.78; R=0.87). This indicates that MSTAR AOT over the study area yielded better results than MOD04 AOT. In conclusion, the aerosol model plays an

AMTD
3, 2651–2680, 2010

important role in the retrieval of AOT, and the use of LUTs based on cluster analysis showed significant potential to retrieve AOT over land. The suggested methodology needs further investigation for the case of bright surface areas. In addition to the SSA and g, the phase function and shape of the aerosol needs to be taken into account. Further analysis with those parameters over study areas could increase the accuracy.

Acknowledgements. The research of K. H. Lee was supported by the Kyungil University Research Grant in 2009. The research of Y. J. Kim was supported by the Korea Meteorological Administration Research and Development Program under Grant CATER 2007-4108. The author would like to thank DAAC/NASA and GSFC/NASA for the use of MODIS and AERONET sun-sky radiometer data.

References

Ackerman, S. A., Strabala, K., Menzel, P., Frey, R., Moeller, C., Gumley, L., Baum, B., Seeman, S. W., and Zhang, H.: Discriminating clear-sky from cloud with MODIS. Algorithm theoretical basis document (MOD35), J. Geophys. Res., 103(D24), 32141–32157, 1998.

AERONET inversion: http://aeronet.gsfc.nasa.gov/new_web/Documents/Inversion_products_V2.pdf, 2010.

AERONET criteria: http://aeronet.gsfc.nasa.gov/new_web/PDF/AERONETcriteria_final1.pdf, 2010.

AERONET: http://aeronet.gsfc.nasa.gov, 2010.

Andrews, E., Sheridan, P. J., Fiebig, M., McComiskey, A., Ogren, J. A., Arnott, P., Covert, D., Elleman, R., Gasparini, R., Collins, D., Jonsson, H., Schmid, B., and Wang, J.: Comparison of methods for deriving aerosol asymmetry parameter, J. Geophys. Res., 111, D05S04, doi:10.1029/2004JD005734, 2006.

d'Almeida, G. A., Koepke, P., and Shettle, E. P.: Atmospheric aerosols: Global climatology and radiative characteristic, A Deepak Publishing, Hampton, Virginia, 561 pp., 1991.

Diner, D., Beckert, J., Reilly, T. H., Bruegge, C., Conel, J. E., Kahn, R. A., Martonchik, J., Ackerman, T. P., Davies, R., Gerstl, S. A. W., Gordon, H., Muller, J.-P., Myneni, R. B., Sellers, P. J., Pinty, B., and Verstraete, M. M.: Multi-angle Imaging SpectroRadiometer (MISR) instrument description and experiment overview, IEEE T. Geosci. Rem. Sens., 36(4), 1072–1087, 1998.

AMTD
3, 2651–2680, 2010

Dubovik, O. and King, M. D.: A flexible inversion algorithm for retrieval of aerosol optical properties from Sun and sky radiance measurements, J. Geophys. Res., 105, 20673–20696, 2000.
Dubovik, O., Smirnov, S., Holben, B. N., King, M. D., Kaufman, Y. J., Eck, T. F., and Slutsker, I.: Accuracy assessment of aerosol optical properties retrieved from AERONET Sun and sky radiance measurements, J. Geophys. Res., 105(D8), 9791–9806, 2000.
Gordon, H. R. and Wang, M.: Retrieval of water-leaving radiance and aerosol optical thickness over the oceans with Sea-WiFS: A preliminary algorithm, Appl. Optics, 33, 443–452, 1994.
Hess, M., Koepke, P., and Schult, I.: Optical Properties of Aerosols and clouds: The software package OPAC, B. Am. Meteorol. Soc., 79, 831–844, 1998.
Holben, B. N., Eck, T. F., Slutsker, I., Tanré,D., Buis, J. P., Setzer, A., et al.: AERONET – A federated instrument network and data archive for aerosol characterization, Rem. Sens. Environ., 66, 1–16, 1998.
Ichoku, C., Kaufman, Y. J., Remer, L. A., and Levy, R.: Global aerosol remote sensing from MODIS, Adv. Space Res., 34, 820–827, 2004.
IPCC: Climate Change: The Science Basis, Cambridge Univ. Press, New York, 870 pp., 2007.
Jeong, M. J., Li, Z., Chu, D. A., and Tsay, S.-T.: Quality and compatibility analyses of global aerosol products derived from the Advanced Very High Resolution Radiometers and the Moderate Imaging Spectroradiometer, J. Geophys. Res., 110, D10S09, doi:10.1029/2004JD004648, 2005.
Kahn, R. A., Gaitley, B. J., Martonchik, J. V., Diner, D. J., Crean, K. A., and Holben, B.: Multiangle Imaging Spectroradiometer (MISR) global aerosol optical depth validation based on 2 years of coincident Aerosol Robotic Network (AERONET) observations, J. Geophys. Res., 110, D10S04, doi:10.1029/2004JD004706, 2005.
Kaufman, L. and Rousseeuw, P. J.: Finding Groups in Data: An Introduction to Cluster Analysis, New York: John Wiley & Sons, Inc., 1990.
Kaufman, Y. J. and Tanré, D.: Algorithm For Remote Sensing of Tropospheric Aerosol from MODIS, Algorithm Theoretical Basis Document, ATBD-MOD-02, NASA Goddard Space Flight Center, 1998.
Kaufman, Y. J., Tanré, D., Remer, L., Vermote, E. F., Chu, A., Holben, B. N.: Operational remote sensing of tropospheric aerosol over the land from EOS-MODIS, J. Geophys. Res., 102(14), 17051–17068, 1997b.
Kaufman, Y. J., Wald, A. E., Remer, L. A., Gao, B. C., Li, R.-R., and Flynn, L.: The MODIS 2.1-

AMTD
3, 2651–2680, 2010

mm channel correlation with visible reflectance for use in remote sensing of aerosol, IEEE T. Geosci. Rem. Sens., 35, 1286–1298, 1997a.

King, D. M., Kaufman, Y. J., Tanre, D., and Nakajima, T.: Remote sensing of tropospheric aerosols from space: past, present, and future, B. Am. Meterol. Soc., 80(11), 2229–2259, doi:10.1175/1520-0477, 1999.

Kinne, S., Schulz, M., Textor, C., Guibert, S., Balkanski, Y., Bauer, S. E., Berntsen, T., Berglen, T. F., Boucher, O., Chin, M., Collins, W., Dentener, F., Diehl, T., Easter, R., Feichter, J., Fillmore, D., Ghan, S., Ginoux, P., Gong, S., Grini, A., Hendricks, J., Herzog, M., Horowitz, L., Isaksen, I., Iversen, T., Kirkevåg, A., Kloster, S., Koch, D., Kristjansson, J. E., Krol, M., Lauer, A., Lamarque, J. F., Lesins, G., Liu, X., Lohmann, U., Montanaro, V., Myhre, G., Penner, J., Pitari, G., Reddy, S., Seland, O., Stier, P., Takemura, T., and Tie, X.: An AeroCom initial assessment – optical properties in aerosol component modules of global models, Atmos. Chem. Phys., 6, 1815–1834, doi:10.5194/acp-6-1815-2006, 2006.

Kokhanovsky, A. A., Breon, F. M., Cacciari, A., Carboni, E., Diner, D., Di Nicolantonio, W., Grainger, R. G., Grey, W. M. F., Höller, R., Lee, K. H., Li, Z., North, P. R. J., Sayer, A., Thomas, G., and von Hoyningen-Huene, W.: Aerosol remote sensing over land: satellite retrievals using different algorithms and instruments, Atmos. Res., 85(3–4) 379–394, doi:10.1016/j.atmosres.2007.02.008, 2007.

Kokhanovsky, A. A., Curer, R. L., de Leeuw, G., Grey, W. M. F., Lee, K. H., Bennouna, Y., Shoemaker, R., and North, P. R. J.: The inter-comparison of AATSR dual view aerosol optical thickness retrievals with results from various algorithms and instruments, Int. J. Rem. Sens., 30(17), 4525–4537, doi:10.1080/01431160802578012, 2009a.

Kokhanovsky, A. A., Deuzé, J. L., Diner, D. J., Dubovik, O., Ducos, F., Emde, C., Garay, M. J., Grainger, R. G., Heckel, A., Herman, M., Katsev, I. L., Keller, J., Levy, R., North, P. R. J., Prikhach, A. S., Rozanov, V. V., Sayer, A. M., Ota, Y., Tanré, D., Thomas, G. E., and Zege, E. P.: The inter-comparison of major satellite aerosol retrieval algorithms using simulated intensity and polarization characteristics of reflected light, Atmos. Meas. Tech. Discuss., 2, 3369–3439, doi:10.5194/amtd-2-3369-2009, 2009b.

Lee, K. H., Li, Z., Kim, Y. J., and Kokhanovsky, A.: Aerosol monitoring from satellite observations: a history of three decades, Atmospheric and Biological Environmental Monitoring, edited by: Kim, Y. J., Platt, U., Gu, M. B., and Iwahashi, H., Springer, 13–38, doi:10.1007/978-1-4020-9674-7, 2009.

Lee, K. H., Kim, Y. J., von Hoyningen-Huene, W., and Burrows, J. P.: Spatio-Temporal Variability

AMTD
3, 2651–2680, 2010

of Atmospheric Aerosol from MODIS data over Northeast Asia in 2004, Atmos. Environ., 41(19), 3959–3973, doi:10.1016/j.atmosenv.2007.01.048, 2007.

Levy, R. C., Remer, L. A., Mattoo, S., Vermote, E. F., and Kaufman, Y. J.: Second-generation operational algorithm: Retrieval of aerosol properties over land from inversion of Moderate Resolution Imaging Spectroradiometer spectral reflectance, J. Geophys. Res., 112, D13211, doi:10.1029/2006JD007811, 2007.

Li, C., Lau, A. K. H., Mao, J., and Chu, A.: Retrieval, validation, and application of the 1-km aerosol optical depth from MODIS measurements over Hong Kong, IEEE Trans. Geosci. Remote Sens., 43(11), 2650–2658, 2005.

Li, Z., Niu, F., Lee, K.-H., Xin, J., Hao, W.-M., Nordgren, B., Wang, Y., and Wang, P.: Validation and understanding of Moderate Resolution Imaging Spectroradiometer aerosol products (C5) using ground-based measurements from the handheld Sun photometer network in China, J. Geophys. Res., 112, D22S07, doi:10.1029/2007JD008479, 2007.

Liu, L. and Mishchenko, M. I.: Toward unified satellite climatology of aerosol properties: direct comparisons of advanced level 2 aerosol products, J. Quant. Spectrosc. Radiat. Transfer, 109(14), 2376–2385, doi:10.1016/j.jqsrt.2008.05.003, 2008.

Mi, W., Li, Z., Xia, X., Holben, B., Levy, R., Zhao, F., Chen, H., and Cribb, M.: Evaluation of the Moderate Resolution Imaging Spectroradiometer aerosol products at two Aerosol Robotic Network stations in China, J. Geophys. Res., 112, D22S08, doi:10.1029/2007JD008474, 2007.

Mishchenko, M. I., Geogdzhayev, I. V., Cairns, B., Carlson, B. E., Chowdhary, J., Lacis, A. A., Liu, L., Rossow, W. B., and Travis, L. D.: Past, present, and future of global aerosol climatologies derived from satellite observations: a perspective, J. Quant. Spectrosc. Radiat. Trans., 106(1–3), 325–347, doi:10.1016/j.jqsrt.2007.01.007, 2007.

Omar, A. H., Won, J.-G., Winker, D. M., Yoon, S.-C., Dubovik, O., and McCormick, M. P.: Development of global aerosol models using cluster analysis of Aerosol Robotic Network (AERONET) measurements, J. Geophys. Res., 110, D10S14, doi:10.1029/2004JD004874, 2005.

Rao, C. R. N., McClain, E. P., and Stowe, L. L.: Remote sensing of aerosols over the oceans using AVHRR data theory, practice, and applications, Int. J. Remote Sens., 10(4–5), 743–749, 1989.

Ricchiazzi, P., Yang, S., Gautier, C., and Sowle, D.: SBDART: A research and teaching software tool for plane-parallel radiative transfer in the Earth's atmosphere, B. Am. Meteorol. Soc.,

AMTD
3, 2651–2680, 2010

79(10), 2101–2114, 1998.
Sheridan, P. J., Delene, D. J., and Ogren, J. A.: Four years of continuous surface aerosol measurements from the Department of Energy's Atmospheric Radiation Measurement Program Southern Great Plains Cloud and Radiation Testbed site, J. Geophys. Res., 106(D18), 20735–20748, 2001.
Shettle, E. P. and Fenn, R. W.: Models for the aerosols of the lower atmosphere and the effects of humidity variations on their optical properties, AFGLTR- 79-0214, US Air Force Geophysics Laboratory, Hanscom Air Force Base, Massachusetts, 1979.
Song, C. H., Park, M. E., Lee, K. H., Ahn, H. J., Lee, Y., Kim, J. Y., Han, K. M., Kim, J., Ghim, Y. S., and Kim, Y. J.: An investigation into seasonal and regional aerosol characteristics in East Asia using model-predicted and remotely-sensed aerosol properties, Atmos. Chem. Phys., 8, 6627–6654, doi:10.5194/acp-8-6627-2008, 2008.
Soufflet, V., Tanré, D., Royer, A., and O'Neill, N. T.: Remote sensing of aerosols over boreal forest and lake water from AVHRR data, Rem. Sens. Environ., 60, 22–34, 1997.
Stowe, L. L.: Cloud and aerosol products at NOAA/ NESDIS, Paleogeogr. Paleoclimatol. Paleoecol., 90, 25–32, 1991.
Streets, D. G., Bond, T. C., Carmichael, G. R., et al.: An inventory of gaseous and 10 primary aerosol emissions in Asia in the year 2000, J. Geophys. Res., 108, 8809, doi:10.1029/2002JD003093, 2003.
von Hoyningen-Huene, W., Freitag, M., and Burrows, J. B.: Retrieval of aerosol optical thickness over land surfaces from top-of-atmosphere radiance, J. Geophys. Res., 108(D9), 4260, doi:10.1029/2001JD002018, 2003.
von Hoyningen-Huene, W., Kokhanovsky, A. A., Wuttke, M. W., Buchwitz, M., Noël, S., Gerilowski, K., Burrows, J. P., Latter, B., Siddans, R., and Kerridge, B. J.: Validation of SCIAMACHY top-of-atmosphere reflectance for aerosol remote sensing using MERIS L1 data, Atmos. Chem. Phys., 7, 97–106, doi:10.5194/acp-7-97-2007, 2007.
Wenig, M., Spichtinger, N., Stohl, A., Held, G., Beirle, S., Wagner, T., Jähne, B., and Platt, U.: Intercontinental transport of nitrogen oxide pollution plumes, Atmos. Chem. Phys., 3, 387–393, doi:10.5194/acp-3-387-2003, 2003.

AMTD
3, 2651–2680, 2010

Table 1. Number of cases in each cluster.

Cluster	Cases	%
1	688	21.4
2	184	5.7
3	1170	36.4
4	814	25.3
5	310	9.7
6	46	1.4
Total	3212	100

AMTD
3, 2651–2680, 2010

Table 2. Summary of aerosol cluster.

	Cluster					
	1	2	3	4	5	6
SSA_{441}	0.915	0.927	0.904	0.908	0.893	0.900
SSA_{675}	0.927	0.941	0.908	0.914	0.939	0.957
SSA_{869}	0.918	0.933	0.897	0.907	0.945	0.964
SSA_{1018}	0.912	0.928	0.889	0.903	0.948	0.966
mr_{441}	1.468	1.478	1.441	1.454	1.508	1.549
mr_{675}	1.480	1.483	1.458	1.472	1.535	1.549
mr_{869}	1.485	1.483	1.468	1.482	1.536	1.537
mr_{1018}	1.481	1.476	1.468	1.481	1.528	1.525
mi_{441}	0.0119	0.0099	0.0127	0.0112	0.0070	0.0049
mi_{675}	0.0086	0.0074	0.0100	0.0088	0.0037	0.0024
mi_{869}	0.0088	0.0078	0.0102	0.0090	0.0036	0.0023
mi_{1018}	0.0091	0.0080	0.0104	0.0092	0.0036	0.0025
g_{441}	0.721	0.729	0.716	0.713	0.730	0.748
g_{675}	0.664	0.685	0.654	0.655	0.693	0.714
g_{869}	0.636	0.657	0.626	0.635	0.691	0.707
g_{1018}	0.626	0.643	0.618	0.634	0.696	0.707
C_{fine}	0.153	0.269	0.079	0.070	0.062	0.130
R_{fine}	0.219	0.257	0.192	0.177	0.162	0.208
S_{fine}	0.531	0.535	0.504	0.474	0.538	0.619
C_{coarse}	0.131	0.192	0.075	0.091	0.346	1.039
R_{coarse}	2.724	2.580	2.915	2.265	2.286	2.241
S_{coarse}	0.583	0.568	0.618	0.656	0.594	0.531

Note that the subscript numbers denote the 441, 675, 869, and 1018 nm wavelengths of the AERONET measurements. "mr" and "mi" are denoting real and imaginary parts of refractive index.The size distribution parameters, volume concentration (C), mean radius (R) and standard deviation (S), are based on a bimodal log normal distribution.

AMTD
3, 2651–2680, 2010

Table 3. Comparison between MSTAR AOT and AERONET AOT at Beijing (116.38 E, 39.98 N) and Xinghe (116.96 E, 39.75 N) for clean, polluted, and dust storm days.

	Beijing			Xinghe		
Case	AERONET	MSTAR	MOD04	AERONET	MSTAR	MOD04
Clean	0.11	0.23	0.31	0.17	0.14	0.06
Polluted	1.09	0.99	1.17	0.99	0.95	0.98
Dust	2.49	2.48	–	2.38	2.18	NA

AMTD
3, 2651–2680, 2010

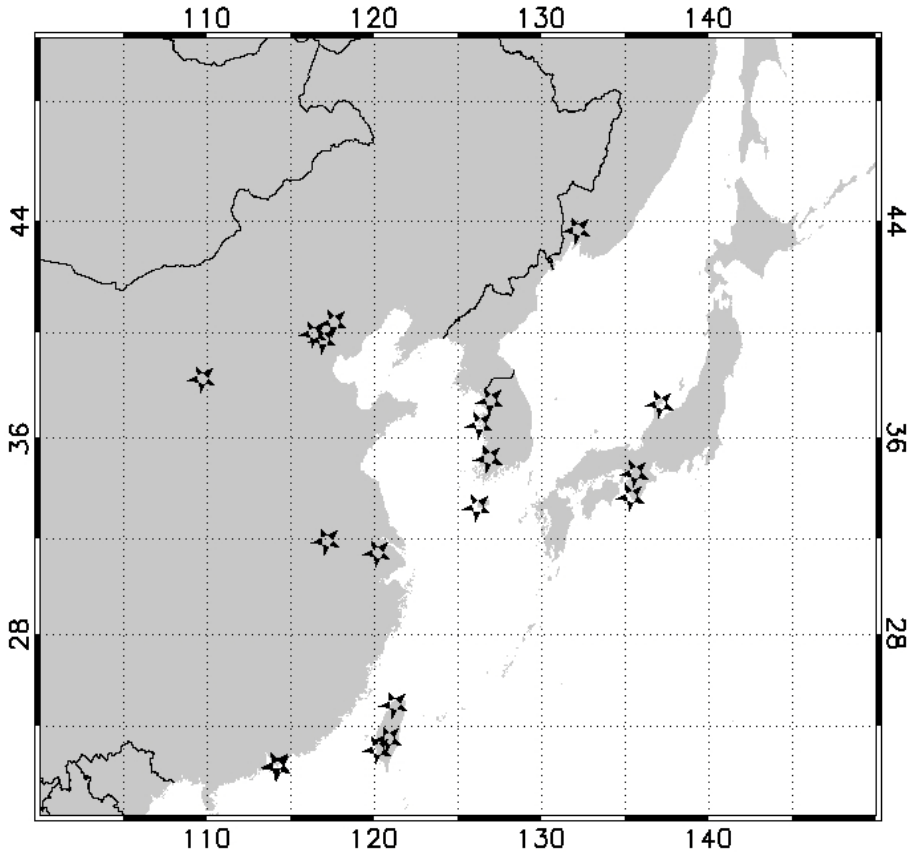

Fig. 1. Map of study area (20~50 N, 100~150 E). Rectangular box represents a sub-area for case study. 20 AERONET sun-sky radiometer measurement sites are shown as star. Geographic locations for each site are available in the AERONET webpage (http://aeronet.gsfc.nasa.gov/).

AMTD
3, 2651–2680, 2010

Satellite remote sensing of Asian aerosols

K. H. Lee and Y. J. Kim

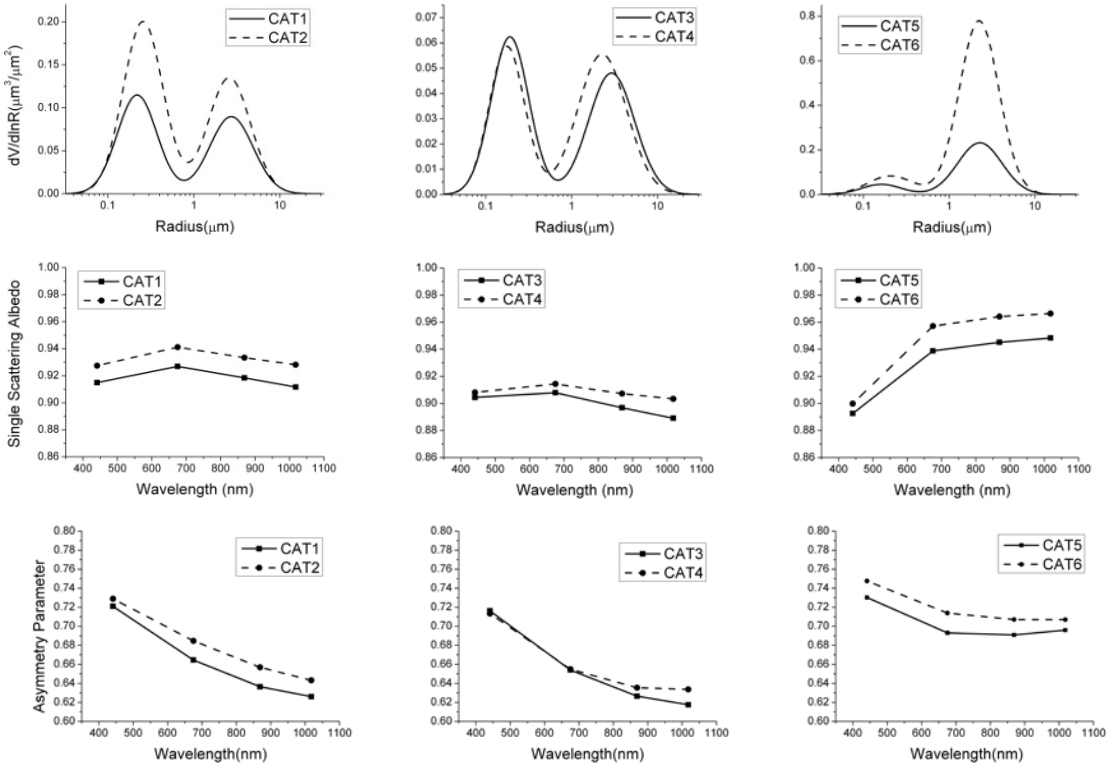

Fig. 2. Aerosol optical and microphysical properties of different types of aerosols classified from the AERONET inversion products.

AMTD
3, 2651–2680, 2010

Satellite remote sensing of Asian aerosols

K. H. Lee and Y. J. Kim

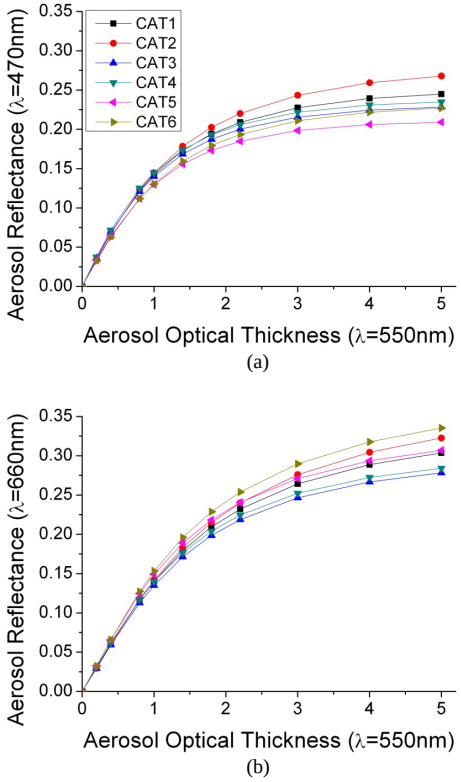

Fig. 3. Aerosol reflectances (**a** λ=470 and **b** 660 nm) as a function of aerosol optical thickness at 550 nm, obtained by SBDART calculations with aerosol models from this study (geometrical inputs are θ_0=60°, θ_S=30°, and Θ=0°). These plots show the increasing of aerosol reflectance for different aerosol model with increasing AOT.

AMTD
3, 2651–2680, 2010

Satellite remote sensing of Asian aerosols

K. H. Lee and Y. J. Kim

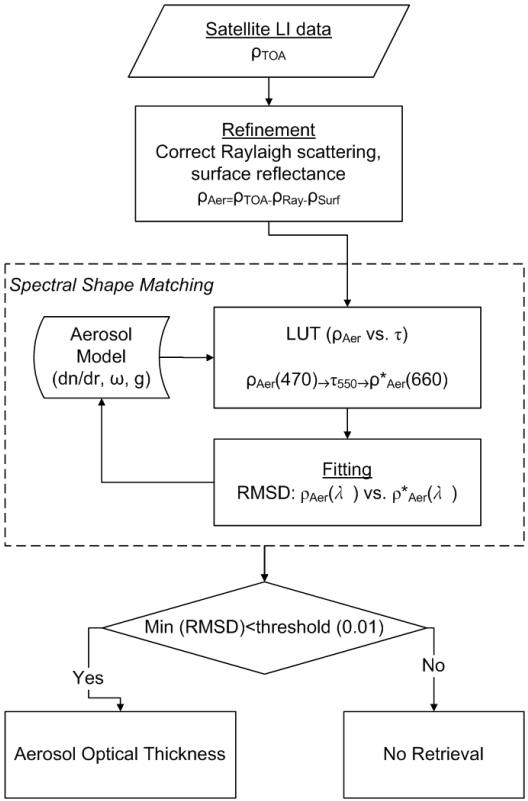

Fig. 4. Schematic diagram of aerosol retrieval.

AMTD
3, 2651–2680, 2010

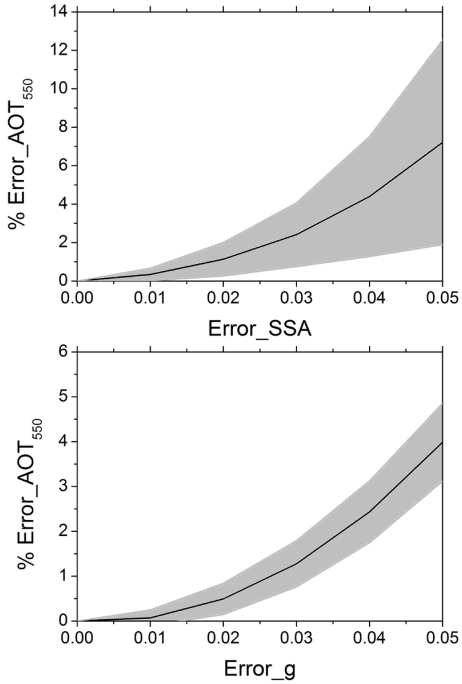

Fig. 5. Percent errors of the retrieved AOT as a function of the error of SSA and g (geometrical inputs are θ_0=60°, θ_S=0°, and Θ=0°). Shaded area shows $\pm\sigma$.

AMTD
3, 2651–2680, 2010

Satellite remote sensing of Asian aerosols

K. H. Lee and Y. J. Kim

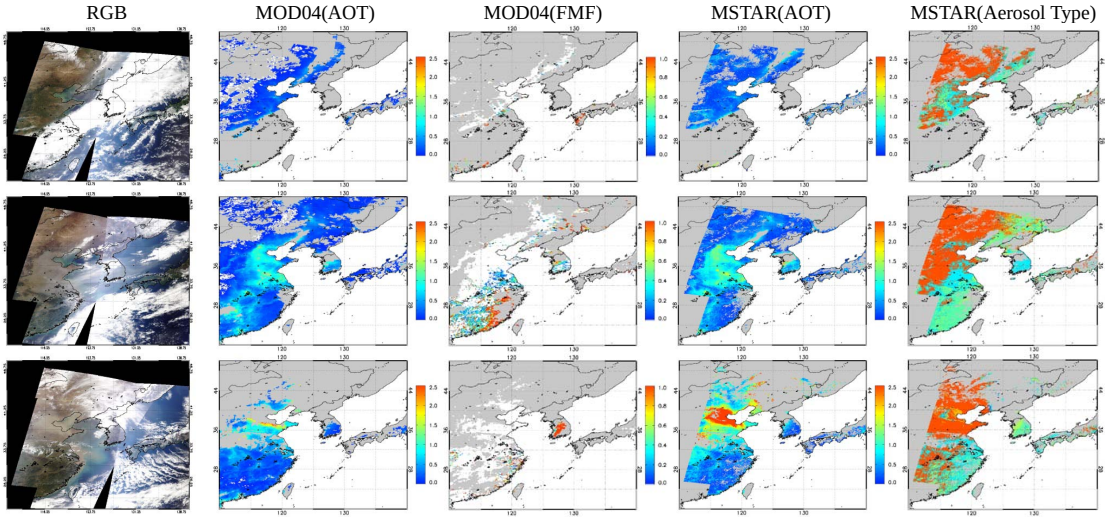

Fig. 6. MODIS RGB color composite image, MSTAR AOT, and collection 5 MOD04 AOT from upper to lower images for (upper) clean case on 21 September, (middle) Pollution case on 23 October, and (lower) Asian dust case on 15 March 2009. Colors for MSRAR aerosol types are red (cat-1), orange (cat-2), yellow (cat-3), green (cat-4), sky-blue (cat-5), and blue (cat-6), respectively.

AMTD
3, 2651–2680, 2010

Satellite remote sensing of Asian aerosols

K. H. Lee and Y. J. Kim

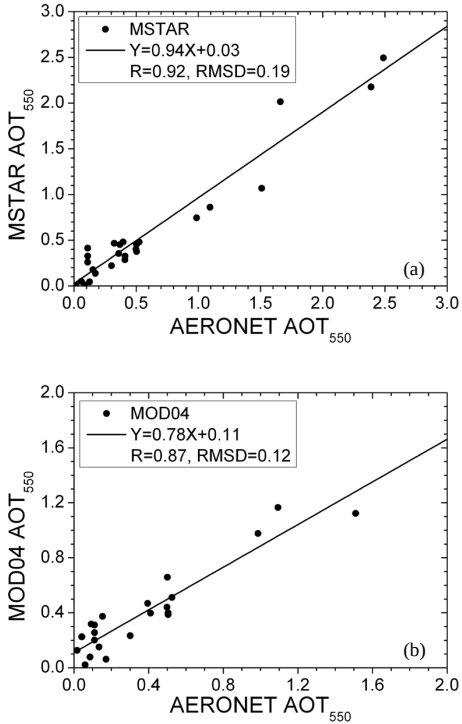

Fig. 7. Comparison of **(a)** MSTAR AOT and **(b)** MOD04 AOT with those measured by AERONET. Effective coincident data numbers are 27 for MSTAR and 22 for MOD04.

AMTD
3, 2651–2680, 2010

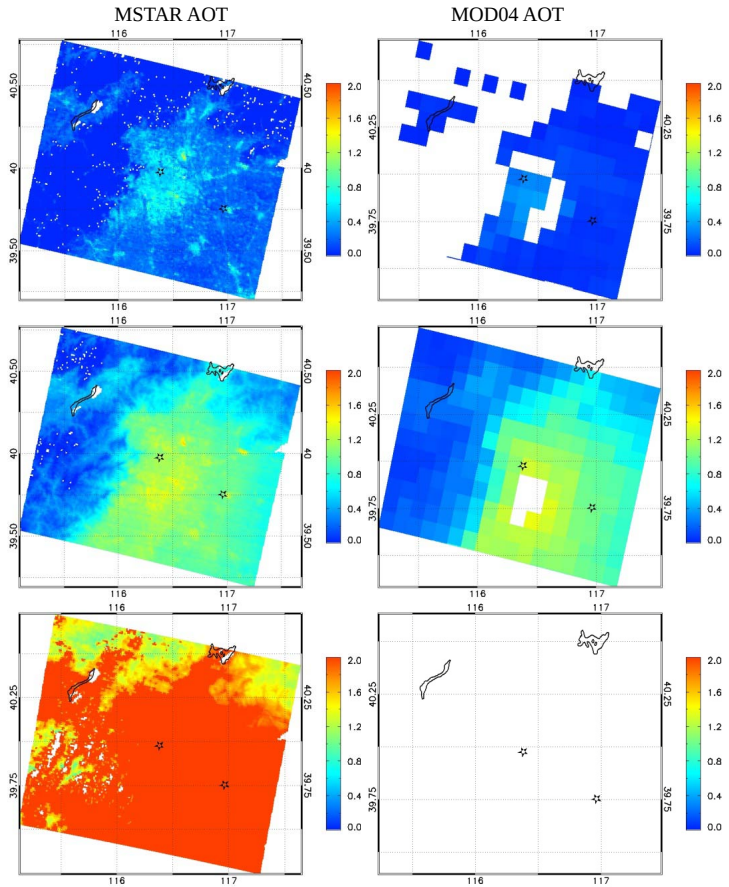

Fig. 8. Case study of clean, pollution, long range transported dust for urban area ($200 \times 100\,km^2$). Note that MOD04 for dust case can't retrieve AOT because of high reflection by dust aerosol.

AMTD
3, 2651–2680, 2010